HHS Public Access

Author manuscript

Mol Cancer Ther. Author manuscript; available in PMC 2022 September 10.

Published in final edited form as:

Mol Cancer Ther. 2021 February ; 20(2): 410–422. doi:10.1158/1535-7163.MCT-20-0316.

EMT-induced gemcitabine resistance in pancreatic cancer involves the functional loss of equilibrative nucleoside transporter 1

Brenna Weadick[1], **Debasis Nayak**[1], **Avinash K. Persaud**[1], **Sau Wai Hung**[2], **Radhika Raj**[1], **Moray J. Campbell**[1], **Wei Chen**[3], **Junan Li**[1], **Terence M. Williams**[4], **Rajgopal Govindarajan**[1,5]

[1]Division of Pharmaceutics and Pharmacology, The Ohio State University College of Pharmacy, Columbus, Ohio.

[2]Department of Pharmaceutical and Biomedical Sciences, University of Georgia, Athens, Georgia.

[3]Department of Pathology, The Ohio State University Wexner Medical Center, Columbus, Ohio.

[4]Department of Radiation Oncology, The Ohio State University Wexner Medical Center, Columbus, Ohio.

[5]Translational Therapeutics, The Ohio State University Comprehensive Cancer Center, Columbus, Ohio.

Abstract

Epithelial-mesenchymal transition (EMT) in cancer cells drives cancer chemoresistance, yet the molecular events of EMT that underpin the acquisition of chemoresistance are poorly understood. Here, we demonstrate a loss of gemcitabine chemosensitivity facilitated by human equilibrative nucleoside transporter 1 (ENT1) during EMT in pancreatic cancer and identify that cadherin switching from the epithelial (E) to neuronal (N) type, a hallmark of EMT, contributes to this loss. Our findings demonstrate that N-cadherin decreases ENT1 expression, membrane localization and gemcitabine transport, while E-cadherin augments each of these. Besides E- and N-cadherin, another epithelial cell adhesion molecule, EpCAM, played a more prominent role in determining ENT1 membrane localization. Forced expression of EpCAM opposed cadherin switching with restored ENT1 expression, membrane localization and gemcitabine transport in EMT-committed pancreatic cancer cells. In gemcitabine-treated mice, EpCAM positive tumors had high ENT1 expression and reduced metastasis, whereas tumors with N-cadherin expression resisted gemcitabine treatment and formed extensive secondary metastatic nodules. Tissue microarray profiling and multiplexed immunohistochemical analysis of pancreatic cancer patient-derived primary tumors revealed EpCAM and ENT1 cell surface co-expression is favored, and ENT1 plasma membrane expression positively predicted median overall survival times in patients treated with adjuvant gemcitabine. Together, our findings identify ENT1 as an inadvertent target of

Corresponding Author: Rajgopal Govindarajan, The Ohio State University College of Pharmacy, 500 W 12th Ave, Columbus, OH 43210. Phone: 614-247-8269 govindarajan.21@osu.edu.

COI statement: The authors declare no potential conflicts of interest.

EMT signaling mediated by cadherin switching and provide a mechanism by which mesenchymal pancreatic cancer cells evade gemcitabine therapy during EMT.

Keywords

ENT; EMT; gemcitabine; resistance; pancreatic cancer; cadherin

INTRODUCTION

Pancreatic cancer remains one of the most devastating malignancies (1). The current standard of care for late stage pancreatic cancer patients relies on chemotherapy including gemcitabine monotherapy and its combinations with 5-fluorouracil, capecitabine or carboplatin, Abraxane®, and FOLFIRINOX, and irinotecan liposome formulations (2,3). In recent years only marginal improvement in patient outcomes has been achieved, primarily due to the development of drug resistance and tumor relapse. Hence, the dismal state of pancreatic cancer treatment outcomes continues, with only ˂10% of patients reaching a 5-year survival time, making it the fourth leading cause of cancer-related deaths (4).

Drug treatment often fails when cancer cells become unresponsive to therapy, yet the mechanisms of resistance acquisition are not fully understood. Recapitulation of epithelial-mesenchymal transition (EMT), a programmed set of interconvertible cellular morphological changes occurring during embryonic ontogeny, is considered a contributing factor for its potential to activate pathways governing cancer chemoresistance (5). EMT also facilitates migration and invasion of cells through the extracellular matrix (6), and multiple independent studies support the importance of EMT for tumor cell dissemination, metastasis, and drug resistance (7–9). Indeed, cancer chemoresistance has been associated with mesenchymal characteristics across many cancer subtypes (10–11), including pancreatic cancer (12–15). The precise mechanism by which mesenchymal pancreatic cancer cells escape drug treatment remains poorly understood.

It is possible that structural modifications implemented by EMT endow cancer cells with characteristics that impair the efficacy of commonly used therapeutic agents. Activation of EMT transcription factors belonging to the ZEB, TWIST, and SNAI1 families have demonstrated the ability to breach epithelial cell integrity to promote de-differentiation associated with poor drug sensitivity. Early in EMT, degradation of tightly maintained epithelial cell-cell contact mediated by tight junctions, adherens junctions, and desmosomes occurs (16). Further, disassembly of the adherens junction by transcriptional repression of epithelial cadherin (E-cadherin) followed by upregulation of neuronal cadherin (N-cadherin), termed cadherin switching, is frequently observed (17). Moreover, epithelial cell adhesion molecule (EpCAM), which regulates proliferation and cell adhesion, is lost in a fraction of circulating tumor cells (CTCs) due to EMT and this correlates with the extent of metastasis occurrence and increased drug resistance (18, 19).

In the current study, we investigated cell junctional changes characteristic of the EMT process and its effect on membrane transport of hydrophilic drugs into cancer cells, the first rate-limiting process determining anticancer efficacy. Specifically, we found the E- to

N-cadherin switching observed during EMT reduces the expression of human equilibrative nucleoside transporter 1 (hENT1), a drug carrier that conducts the membrane transport of gemcitabine in pancreatic cancer cells. EpCAM, on the other hand, substantially augments hENT1 cell surface expression and enhances sensitivity to gemcitabine in pancreatic cancer cells by opposing cadherin switching. In both mice harboring orthotopic pancreatic tumor xenografts and human pancreatic cancer patients, EpCAM principally determined ENT1 cell surface localization, gemcitabine treatment response, and survival outcomes. Together, our findings identify that hENT1 is an inadvertent target of EMT signaling mediated by cadherin switching and provide a mechanism by which mesenchymal pancreatic cells evade drug therapy during the EMT process.

MATERIALS AND METHODS

Cell Culture

The pancreatic ductal adenocarcinoma cell line, PANC-1, was obtained from American Type Culture Collection (ATCC Cat# CRL-1469, RRID:CVCL_0480) and maintained in Dulbecco's Modified Eagle Medium (DMEM) supplemented with 10% FBS. PANC-1 cells were subcultured at a 1:8 ratio and used within 25 passages. Epithelial and mesenchymal subpopulations of cells were isolated from PANC-1 cells (N+/E− and E+/N− cells), and cultured under the same conditions as parental PANC-1 cells. All experiments were conducted within the tenth passage of the clones to avoid risk of further transformation and loss of isogenicity. MIA PaCa-2 (ATCC Cat# CRL-1420, RRID:CVCL_0428), HPAF-II (ATCC Cat# CRL-1997, RRID:CVCL_0313), and Capan-1 (ATCC Cat# HTB-79, RRID:CVCL_0237) cell lines were obtained from ATCC. ATCC uses morphological, cytogenetic and DNA profile analysis for characterization of cell lines. A431D, A431D-E and A431D-N cells were generously provided by Dr. Parmender P. Mehta (University of Nebraska Medical Center) and maintained as described before (20). All cells were incubated in 5% CO_2 at 37°C. Routine mycoplasma testing was performed on cell lines in this study with R&D Systems' MycoProbe Mycoplasma Detection Kit, with the latest screening conducted 8/26/20.

Orthotopic Pancreatic Tumor Xenograft Implantation and Gemcitabine Treatment

For *in vivo* studies, 8-week-old female athymic nude mice were received from the Jackson Laboratory (IMSR Cat# JAX:007850, RRID:IMSR_JAX:007850). Procedures were performed in accordance with our protocol 2015A00000095-R1 approved by The Ohio State University Institutional Animal Care and Use Committee and animals were maintained in facilities approved by the Association for Assessment and Accreditation of Laboratory Animal Care International, the Office of Laboratory Animal Welfare, and in compliance with the United States Department of Agriculture standards and regulations. After one week of acclimatization, mice were randomly caged into groups of 5. For orthotopic implantation of pancreatic cancer cell lines, all the procedures were carried out under a biosafety cabinet. Mice were anesthetized by 3% isoflurane inhalation initially and then 1% isoflurane was maintained throughout the surgical procedure. The abdominal area of mice was cleaned with povidone iodine solution thrice and a 1 cm incision was made at the upper left quadrant of the abdominal cavity. Human pancreatic cancer cell lines: PANC-1, E+/N−, N+/E−, PANC-1

OE EpCAM, or PANC-1 OE N-cad (2×10^5 cells suspended in 50 μL of sterile PBS and 50% v/v Matrigel) were injected into the tail region of the pancreas, avoiding any major blood vessels and spillage into the peritoneal cavity. Skin incisions were closed by sterile absorbable surgical sutures and wounded area was cleaned with povidone iodine solution. Isoflurane was then removed, and mice were administered 100% oxygen (1–2 min) for their recovery. Analgesic medication (0.5 mg/mL meloxicam) was given subcutaneously every 24 h for 3 subsequent days post-surgery. Two weeks after orthotopic injection, gemcitabine treatment was commenced by intraperitoneal (IP) injection (25 mg/kg) and continued twice a week for the duration of the study. Mice were monitored daily following surgery to ensure proper wound healing and weighed twice a week throughout the course of the experiment. Twelve weeks after orthotopic injection mice were euthanized. Primary tumors were weighed. Tumor dimensions were measured by a Vernier Caliper and calculated using the following formula: tumor volume= $\pi/6$ (L × S × S), where L= longest diameter and S = the shortest tumor diameter. Additionally, metastatic foci were counted in the liver, spleen, kidney, intestine, and peritoneum by examination under a stereo Zoom (10X) microscope.

TMA Construction

A tissue microarray comprising of tumor samples from 114 patients with pancreatic cancer was generated under an IRB protocol (2014C0077) approved by The Ohio State University. Tumor samples were collected from pancreatectomy procedures. Specifically, pancreaticoduodenectomy procedures were performed for tumors located in the pancreas head region and distal pancreatectomy with splenectomy procedures were performed for tumors in the pancreas tail region. Formalin-fixed paraffin embedded representative tumor blocks were selected by evaluation of hematoxylin & eosin stained slides by a board-certified gastrointestinal pathologist (Dr. Wei Chen), and cores drawn from viable, non-necrotic regions of tumor with a 1.5 mm coring needle using a Pathology Devices Arrayer (San Diego, CA). Tumor tissue cores were placed in duplicate (along with normal adjacent pancreas tissue for 25 patients) into three paraffin blocks. After all cores were placed into the paraffin block, the microarray blocks were gently heated in a 40°C oven for approximately 45 minutes to fuse the cores to the paraffin within the block. Microarrays were then sectioned and stained. A clinically-annotated database summarizing the demographics, clinical-pathologic characteristics, and clinical outcomes for each patient was developed by Dr. Terence Williams. All patients were treated with surgical resection with or without post-operative chemotherapy, which largely consisted of gemcitabine-based chemotherapy. The demographic information for TMAs is provided in Table I.

Other Methods: Plasmids, Antibodies, Reagents, Flow Cytometry, Colony Formation Assay, Expression of E-cadherin, N-cadherin, and EpCAM, [5-^{3}H] Gemcitabine Transport Assay, Western Blotting, Transwell Migration and Invasion Assays, Pathway and gene set enrichment analysis of deposited RNA-sequencing data, Multiplexed Fluorescent Immunohistochemistry, TMA Quantification, Statistical Analysis, Immunocytochemistry (See Supplemental Materials)

RESULTS

1. Isolation and characterization of epithelial and mesenchymal human pancreatic cancer cells

To study the molecular modifications that occur during the EMT process in pancreatic cancer, we developed a cell-based EMT model system. First, several isogenic epithelial (E-cadherin enriched /N-cadherin depleted; E+/N−) and mesenchymal (N-cadherin enriched/E-cadherin depleted; N+/E−) clones were isolated from the parental PANC-1 cell line through flow cytometry cell sorting and clonal expansion (Fig. S1A–D). Immunostaining confirmed that the expression of N-cadherin and E-cadherin were greatly enriched in N+/E− and E+/N− cells, respectively, compared to PANC-1 cells (Fig. S2A). E+/N− and N+/E− clones were characterized by established *in vitro*, biochemical and *in vivo* models. Epithelial clones displayed tight cell-cell adhesion and smooth colony morphology, whereas, mesenchymal clones displayed loose cell-cell contact, elongated cellular morphology and rough colony edges (Fig. S2B). Increased protein expression of epithelial markers E-cadherin and ZO-1 was evident in epithelial clones, whereas, mesenchymal clones exhibited high expression of the mesenchymal markers N-cadherin, β-catenin, Vimentin, SLUG and ZEB-1 (Fig. S2C). Proliferation was measured in each cell type, and E+/N− cells showed slightly decreased in growth up to 72 h compared to PANC-1 cells, while N+/E− cells grew faster at time points beyond 72 h (Fig. S2D). A Matrigel invasion assay was performed, and mesenchymal clones demonstrated greater migratory capabilities compared to epithelial and PANC-1 clones (Fig. S2E). Additionally, mesenchymal cells showed increased migration as determined by a transwell migration assay (Fig. S2F). To ensure the stability and isogenicity of the clones, the above characterization experiments were repeated several times. E+/N− and N+/E− clones, which retained purity after multiple passages (Fig. S1E), were used for conducting subsequent experiments. Mesenchymal clones, compared to the epithelial clones and PANC-1, led to significantly increased tumor burden and metastases to the liver, spleen, kidney, and intestines in athymic nude mice bearing orthotopic pancreatic tumor xenografts (Fig. S2G–I; Fig. S3A–C). Furthermore, the ability of gemcitabine to inhibit mesenchymal clone-induced pancreatic tumor growth and metastases in athymic nude mice was reduced compared to the epithelial clones and PANC-1 (Fig. S2J–L; Fig. S3D–F). This model was shown to be consistently stable and effectively represents epithelial and mesenchymal states of EMT in pancreatic cancer. In support of other data, mesenchymal sub-types of pancreatic cancer cells are aggressive in nature, highly metastatic, and less responsive to chemotherapy.

2. Epithelial and mesenchymal cells display contrasting ENT1 expression, cell surface localization and transport activity

Previously, we and others have demonstrated that ENT1 conducts low-affinity, high-capacity membrane transport of hydrophilic nucleoside analog drugs into pancreatic cancer cells (21–23). To explore how EMT-induced alterations may contribute to the observed differences in gemcitabine sensitivity, we evaluated the expressional and functional characteristics of ENT1 in E+/N− and N+/E− clones. ENT1 protein expression was decreased in N+/E− cells, while enhanced in E+/N− cells compared to parental PANC-1 cells (Fig. 1A). Notably, the loss of ENT1 expression coincides with reduced epithelial characteristics or increased mesenchymal characteristics, or both, observed during EMT. ENT1 is primarily found at

the basolateral cell surface in polarized epithelial cells in accordance with its involvement in vectorial transport of nucleosides in cells (24). Consistently, lateral localization of ENT1 in PANC-1 cells was confirmed by co-staining with E-cadherin, an integral component of adherens junctions which form at lateral cell-cell connections (Fig. 1B, Supplemental file 1). Immunocytochemical analysis showed disorganization of ENT1 at cell-cell contacts with reduced expression in N+/E− cells, but PANC-1 and E+/N− cells displayed moderate to high levels of ENT1 localization at cell-cell contacts (Fig. 1C). Orthogonal perspectives of Z-projection images showed that ENT1 is clearly localized at the lateral surface in PANC-1 and basolateral membrane in E+/N− cells, while increasingly accumulated in the cytosol with reduced lateral membranous expression in N+/E− (Fig. 1D). Imaris software animation of Z-stack 3D reconstructions likewise display mislocalization of ENT1 in N+/E− cells (Supplemental files 2–4).

To determine the functional consequences of reduced expression and mislocalization of ENT1 in N+/E− cells, we performed a radioligand transport study to examine ^{3}H-gemcitabine transport into N+/E− and E+/N− cells. Transport was measured for one minute, and figure 1E shows ^{3}H-gemcitabine accumulation was reduced in N+/E− compared to PANC-1 cells and E+/N− cells. A colony formation assay was performed to determine the impact of ENT1 mislocalization on gemcitabine sensitivity over a more extended time frame. Figure 1F shows that after three weeks of gemcitabine treatment (10 nM), a greater number of N+/E− cells were able to resist gemcitabine-induced cytotoxicity. Collectively, these findings demonstrate that mesenchymal traits are associated with decreased ENT1 expression, mislocalization and reduced gemcitabine transport, suggesting that changes in ENT1 observed during the EMT process may contribute to loss of gemcitabine sensitivity.

3. E-cadherin augments ENT1, while N-cadherin expression reduces ENT1 at the cell surface leading to decreased gemcitabine sensitivity

Upon determining the mislocalization of ENT1 and loss of gemcitabine transport function during EMT, we next sought to investigate EMT-altered pathways in the context of pancreatic cancer which could potentially modulate ENT1. Utilizing a previous study by Takahashi *et al.* which demonstrated that serial orthotopic implantation of PANC-1 cells induced EMT and conferred highly malignant traits to primary tumor and liver metastasis derived cell lines (25), we performed bioinformatic analysis of RNA sequencing data sets comparing parental PANC-1 and PANC-1 liver metastasis. Unbiased pathway and gene set analysis identified actin filament and bundle organization as highly altered gene ontology pathways, along with cell substrate junction, protein containing complex disassembly, and regulation of binding (Fig. S4A). Consistent with this finding, immunostaining for ENT1 and actin showed a severe disruption of the actin cytoskeleton in N+/E− cells, but intact structures with filamentous actin at the cell periphery in E+/N− cells (Fig. S4B). Intriguingly, Takahashi and colleagues demonstrated that alteration of actin cytoskeletal organization coincided with loss of E-cadherin in PANC-1 liver metastasis cells (25).

Upon these observations, we sought to investigate the influence of E to N-cadherin switching, a structural change characteristic of EMT, on ENT1 expression and function. E-cadherin was overexpressed in PANC-1 cells, and ENT1 protein levels increased (Fig.

2A). ENT1 cell surface expression was enhanced in PANC-1 cells overexpressing E-cadherin, in subconfluent conditions (Fig. 2B). On the other hand, overexpression of N-cadherin decreased ENT1 protein levels and cell surface localization even in confluent conditions (Fig. 2C/D). Similar results were obtained in N+/E− and E+/N− cells following overexpression of E-cadherin and N-cadherin, respectively (Fig. S5A, B). To determine if cadherin switching modulates ENT1 expression in a similar fashion in other pancreatic cancer lines, we overexpressed E-cadherin and N-cadherin in MIA PaCa-2, Capan-1, and HPAF-II cells and obtained similar results (Fig. S6A, B). Functionally, forced expression of E-cadherin did not change ^{3}H-gemcitabine accumulation in PANC-1 cells (Fig. 2E), but significantly increased ^{3}H-gemcitabine accumulation N+/E− cells (Fig. 2F), suggesting that E-cadherin positively influences ENT1 transport function. Oppositely, N-cadherin overexpression resulted in a non-statistically significant decrease in the accumulation of ^{3}H-gemcitabine in PANC-1 ($p= 0.057$) (Fig. 2G) and E+/N− cells (Fig. 2H). To further investigate the negative impact of N-cadherin on gemcitabine accumulation, PANC-1 and PANC-1 N-cadherin overexpressing cells were treated with gemcitabine (10 nM) for three weeks and analyzed for colony formation. The results show that N-cadherin overexpression conferred resistance to gemcitabine cytotoxicity, with a greater number of colonies sustained growth despite the presence of gemcitabine (Fig. 2I).

To probe the necessity of E-cadherin for ENT1 plasma membrane localization, A431D cells, which are null for both E-cadherin and N-cadherin and derived from the epidermoid carcinoma cell line A431, were examined (20). Immunocytochemical analysis showed ENT1 was retained at the cell surface even in the absence of E-cadherin, although E-cadherin overexpression did augment ENT1 protein levels (Fig. S6C). Immunocytochemistry confirmed A431D E-cadherin overexpression cells had further increased ENT1 levels at the cell surface, supporting a positive influence of E-cadherin on ENT1 cell surface localization; conversely, forced N-cadherin expression in A431D diminished ENT1 at the cell surface (Fig. S6D). These results indicate that E- to N-cadherin switching significantly influences ENT1, evidenced by E-cadherin augmentation of ENT1 and N-cadherin depletion of ENT1. Nonetheless, E-cadherin is not essential for ENT1 to function at the cell surface of cancer cells, as significant plasma membrane accumulation of ENT1 was observed without detectable E-cadherin expression.

4. EpCAM opposes cadherin switching and restores ENT1 cell surface expression and transport activity

The cell surface localization of ENT1 in cadherin null A431D cells caused us to consider other factors that could promote epithelial integrity. Interestingly, expression of the epithelial cell adhesion molecule EpCAM was observed at the cell surface of A431D cells and appeared to colocalize with ENT1 (Fig. S6E). Therefore, we proposed that cancer cells which have suppression of E-cadherin may retain ENT1 function at the cell surface due to EpCAM's positive influence. Stable overexpression of EpCAM in PANC-1 cells was performed and ENT1 protein levels were increased in PANC-1 cells overexpressing EpCAM (Fig. 3A). Both EpCAM and ENT1 were prominently organized at the cell surface upon EpCAM overexpression, suggesting that EpCAM promotes accumulation of ENT1 at the cell surface (Fig. 3B). Further, the positive influence on ENT1 was not limited to

cells with EpCAM overexpression, evidenced by the meticulous membrane expression of ENT1 in cells lacking EpCAM staining (Fig. 3B). It is possible that EpCAM expression augments the assembly of other cell surface junctional proteins that may support ENT1 by promoting epithelial integrity, producing a “bystander effect” in neighboring cells. Previous studies in our laboratory have uncovered the positive influence of E-cadherin on Connexin 43 assembly in gap junctions, which supports this notion (26). Distinct lateral membrane colocalization of ENT1 and EpCAM was displayed by Z-projection images (Fig. 3C) and 3D reconstruction of Z-stacks (Supplemental file 5) of PANC-1 cells overexpressing EpCAM, which represent cells grown in a monolayer. Similarly, EpCAM was overexpressed in EMT-committed N+/E− cells that are devoid of both EpCAM and E-cadherin, and interestingly, only those cells that expressed EpCAM displayed ENT1 at the cell surface (Fig. 3D). The ^{3}H-gemcitabine transport capacity was unaffected in PANC-1 cells overexpressing EpCAM (Fig. 3E), whereas, cell surface accumulation of ENT1 increased and restored ENT1 mediated transport in N+/E− cells overexpressing EpCAM (Fig. 3F). Furthermore, to determine if EpCAM may exert its stabilizing influence on ENT1 by modulating the expression of E-cadherin and/or N-cadherin, Western blotting analysis of PANC-1 and N+/E− cells overexpressing EpCAM was performed. Figure 3G shows E-cadherin expression was increased due to EpCAM overexpression, and N-cadherin protein levels were decreased. Collectively, these findings indicate the importance of EpCAM for proper ENT1 cell surface localization and transport activity in PANC-1 cells and suggest the effects are mediated, at least partially, by opposing the negative influence of cadherin switching.

5. N-cadherin-positive tumors evade gemcitabine drug therapy in an orthotopic mouse model of pancreatic cancer

ENT1 is a primary determinant of tumor cell sensitivity to nucleoside analog drugs (21–23, 27). Having demonstrated N-cadherin reduces ENT1 at the cell surface and EpCAM enhances ENT1, we next examined how the expression of these cell adhesion molecules would affect tumor size and metastatic burden after gemcitabine treatment in tumor-bearing mice. An equivalent cell number of PANC-1, PANC-1 N-cadherin overexpression and PANC-1 EpCAM overexpression cells were orthotopically injected into the pancreas of 8-week-old female athymic nude mice. Two weeks after injection, gemcitabine was administered (25 mg/kg IP) and continued twice weekly for the duration of the experiment, schematically displayed in Figure 4A. Body weight was measured weekly for each animal, and no significant weight loss was observed during gemcitabine treatment (Fig. S7). Mice were sacrificed to evaluate both the primary tumor and formation of metastatic foci twelve weeks after orthotopic injections. Notably, three of the five mice with N-cadherin positive tumors were sacrificed prior to the twelve-week endpoint (two at week 8, and one at week 10) as early removal criteria were met due to excessive tumor burden. Tumors generated with N-cadherin overexpressing cells formed larger tumors than PANC-1 cells, and the EpCAM overexpression tumors had the least weight and volume among the three groups (Fig. 4B). Pancreatic cancer often forms metastases in nearby organs such as the liver and peritoneum. Thus, we tallied gross metastatic foci in the liver, spleen, peritoneum, kidney, and intestines. A significantly greater number of metastatic foci were observed in N-cadherin overexpression tumors, with intermediate metastases in PANC-1 tumors, and

the least incidence in EpCAM overexpression tumors (Fig. 4C/D). To evaluate whether the expression of ENT1 influenced gemcitabine treatment outcomes, immunohistochemical analysis was performed on mouse tumor specimens after the completion of treatment. We found that ENT1 was highly expressed in EpCAM overexpression tumors compared to N-cadherin overexpression tumors (Fig. 4E), demonstrating EpCAM and ENT1 co-expression correlates with decreased tumor burden and metastases. ENT1 was diminished in N-cadherin overexpression tumors, especially in regions where high expression of N-cadherin was observed (Fig. 4F).

6. Cell surface ENT1 localization is influenced by N-cadherin and EpCAM expression in human pancreatic cancer

Tissue microarray (TMA) analysis of patient-derived pancreatic ductal adenocarcinoma (PDAC) samples (n=114) and adjacent normal pancreatic tissues (n=25) was performed. Notably, we prepared TMAs from pancreatic cancer patients representing different stages of the disease, all treated surgically with or without postoperative chemotherapy treatment which consisted of primarily gemcitabine monotherapy or gemcitabine-based combinations (Supplemental Table 1). Univariate survival analysis of demographic and clinical parameters revealed that treatment with adjuvant chemotherapy favored improved patient outcomes with a median overall survival time of 677 days and 383 days with and without treatment, respectively (Table 1, Fig. S8). Extensive primary tumor growth (T stage= 3/4), presence of regional lymph node spread (N stage= 1), and positive surgical margin status were also significantly associated with decreased overall survival time (Table 2).

Multiplexed immunohistochemistry staining was performed, and ENT1 staining was observed in hyperplastic tumor regions in a portion of patients, while not detectable in others with a range of variable staining in between (Fig. S9). Representative images showed ENT1 is distinctly expressed at the plasma membrane of EpCAM-positive cells (Fig. 5A), whereas, cytosolic ENT1 or absence of ENT1 was observed in tumor cells with plasma membrane expression of N-cadherin (Fig. 5B). Tumor cells were categorized and counted by inForm™ software based on the expression of ENT1 and EpCAM plasma membrane coexpression (double positivity) or individual expression (single positivity). Fewer cells were positive for ENT1 or EpCAM alone, suggesting that coexpression of ENT1 and EpCAM is favored (Fig. 5C). Likewise, ENT1 and N-cadherin positive/negative expression in tumor cells was computed, and a greater proportion of cells were double positive for both cytoplasmic ENT1 expression and N-cadherin plasma membrane expression (Fig. 5D). Cell segmentation divided tumor cells in each image into cytoplasmic and plasma membrane compartments (Fig. S10/S11), and a positive correlation in plasma membrane expression of ENT1 and EpCAM was noted ($r=0.52$; $p < 0.001$) (Fig. 5E). Further, plasma membrane N-cadherin correlated with cytoplasmic localization of ENT1 ($r=0.45$; $p < 0.001$) (Fig. 5F). These data indicate the importance of cell adhesion molecule expression for supporting or diminishing cell surface ENT1 in human pancreatic cancer, which directly impacts drug accumulation in tumor cells.

7. ENT1 cell surface localization predicts survival outcome in gemcitabine treated pancreatic cancer patients

To determine if subcellular localization of ENT1 affects patient survival, ENT1 was quantified specifically in the plasma membrane compartment based on fluorescent signal intensity to produce an H-score ranging from 0–300 (see Methods). The median H-score was 96.1, so we chose 100 as a threshold value to categorize high and low expression of membrane ENT1. As ENT1 is a determinant of drug sensitivity, we examined how membrane expression of ENT1 influenced survival outcomes among treated patients (97 out of 114 patients, 85.1%). Adjuvant chemotherapy is the standard of care for pancreatic cancer patients, so it is expected that treated patients were the vast majority of cases. The median overall survival time for patients with H-score < 100 was 634 days (95% CI [541, 727]), and the corresponding time for patients with H score ≥ 100 was 840 days (95% CI [693, 987]), and univariate survival analysis demonstrated that high plasma membrane ENT1 (H-score ≥100) favors median overall survival (Fig. 5G, Table 1). Multivariate survival analyses confirmed that ENT1 membrane H-score, chemotherapy, and tumor N stage were significantly associated with overall survival in an independent manner (for H score ≥ 100 *vs.* H score < 100, with chemotherapy *vs.* without chemotherapy, and N stage 1 *vs.* 0) (Table 1). Because N stage and T stage were so closely associated ($p < 0.001$), and T stage was unevenly represented in this patient cohort (T stage 1/2, n=105; T stage 3/4, n=9), N stage was included in the final multivariate analysis. Together, these findings suggest that EpCAM-supported, cell surface ENT1 localization is an important predictor of overall survival in patients treated with gemcitabine. Besides overall survival, we found associations between ENT1 H-score >100 and N stage of 0 ($p=0.027$) and T stage of 1/2 ($p=0.034$), indicating that cell surface ENT1 correlates with absence of regional lymph node spread and limited primary tumor growth at the time or surgical resection.

DISCUSSION

In this study, we investigated how cell adhesion molecules regulated by the EMT program confer resistance to nucleoside analog chemotherapy in pancreatic cancer. Our findings demonstrate that cadherin switching initiated by EMT negatively influences ENT1 expression, cell surface localization, and transport function in epithelial pancreatic cancer cells resulting in gemcitabine resistance. In addition, EpCAM opposed cadherin switching resulting in restoration of ENT1 function and gemcitabine sensitivity. Analysis of gemcitabine-treated orthotopic tumor-bearing mice demonstrated that tumors with breached ENT1 function due to forced expression of N-cadherin were less responsive to gemcitabine therapy, had higher tumor burden, and had greater incidence of metastasis. Furthermore, immunohistochemical subtyping of pancreatic cancer patient-derived samples revealed EpCAM and ENT1 cell surface coexpression is favored, and plasma membrane-localized ENT1 positively predicted median overall survival times in patients that received gemcitabine-based chemotherapy. Together, our study identifies a putative mechanism by which EMT-committed cells lose sensitivity to nucleoside analog chemotherapeutic agents during pancreatic cancer progression.

Coordinated phenotypic changes initiated by EMT convert a subpopulation of epithelial tumor cells into mesenchymal-like cells, providing cancer cells with the ability to disseminate and resist chemotherapy. Although tumor cells exist in a plethora of intermediate states possessing varying levels of both epithelial and mesenchymal traits (28), isolation and expansion of isogenic PANC-1 sublines based on differential expression of E-cadherin and N-cadherin allowed for comparison between representative epithelial and mesenchymal-type pancreatic cancer cells *in vitro*. The observed reduction and/or mislocalization of ENT1 in mesenchymal cells led us to consider the potential influence of molecular alterations built into the EMT program. Classical cadherins form adherens junctions that contribute to epithelial integrity which is lost in EMT (14) and may be important for cell surface expression of transmembrane proteins like ENT1. Further, cadherin switching is noted alongside activation of EMT signaling pathways in many solid tumors (29, 30) and silencing of EMT transcription factors Snail and Twist resulted in increased expression of ENT1 (11). Therefore, we hypothesized that cadherin switching may have an integral role in regulating ENT1 expression.

Interestingly, across four different pancreatic cancer cell lines we found that forced expression of E-cadherin was accompanied by increased ENT1 protein levels. Further examination of the PANC-1 cell line expressing E-cadherin showed enhanced cell-cell contact and membrane staining of ENT1, suggesting that partial restoration of the epithelial phenotype promotes proper localization and function of ENT1. Opposite results were obtained when N-cadherin was overexpressed in epithelial pancreatic cancer cells, along with the aforementioned loss of ENT1 expression and mislocalization. Regarding ENT1 functionality, our results indicate that the greater the amount of E-cadherin expression in each respective cell line, the more resistant to changes in gemcitabine transport upon forced expression of an exogenous gene. Indeed, the only statistically significant changes we observed were in cells with no E-cadherin expression (N+/E− cells), when E-cadherin or EpCAM was overexpressed. These findings point to the importance of epithelial adhesion molecules that maintain epithelial integrity for ENT1 functionality, and the ability of E-cadherin retention to minimize the effects of N-cadherin expression in scenarios when both are expressed.

Previous studies have investigated the loss of E-cadherin in PANC-1 cells. Takahashi and colleagues recently demonstrated that orthotopic implantation of PANC-1 cells resulted in decreased expression of E-cadherin, suggesting that the pancreatic cancer tumor microenvironment affects E-cadherin (25). This is supported by earlier work by Menke and colleagues which found that PANC-1 cells co-cultured with collagen, a major component of the extracellular matrix abundant in the desmoplastic stroma characteristic of pancreatic cancer, led to downregulation of E-cadherin (31). Despite the indication that the TME plays a role in loss of E-cadherin to promote EMT, the mechanisms of loss of ENT1 during this process is unclear. It is well known that the cytoskeleton is greatly altered during the EMT process to accommodate sweeping morphological changes and migratory capabilities. An earlier study demonstrates colocalization of ENT1 and F-actin at the cell surface and loss of cell surface accumulation of ENT1 after pharmacological disruption of actin polymerization (32). Further, adherens junctions rely on actin to form secure cell-cell attachments (cadherins are linked to the actin cytoskeleton by β-catenin and α-catenin).

Therefore, disruption of adherens junctions (downregulation of E-cadherin), dismantling of cell adhesion complexes, and/or reorganization of the actin cytoskeleton, all observed during EMT, may be responsible for the loss of ENT1 cell surface accumulation in mesenchymal cells. To investigate this possibility further, we performed bioinformatic analysis of the RNA sequencing data from the study conducted by Takahashi and colleagues (25), mentioned above, which demonstrated that orthotopic implantation of PANC-1 cells permitted to grow in the TME resulted in loss of E-cadherin in primary tumors and PANC-1-derived liver metastasis. Intriguingly, gene set enrichment analysis revealed that organization of the actin cytoskeleton, along with cell substrate junction, protein containing complex disassembly, and regulation of binding, was altered in PANC-1 liver metastasis compared to primary tumor cells. Immunocytochemical analysis of actin and E-cadherin further confirmed this occurrence in mesenchymal PANC-1 cells isolated in this study. Taken together, these findings support the notion that structural changes during the EMT process (disruption of cell junctional complexes and reorganization of the actin cytoskeleton) is a possible mechanism by which proper cell surface tethering of ENT1, required for gemcitabine uptake, is compromised.

EpCAM is expressed in numerous epithelia and epithelial-derived neoplasms and has been shown to play a complex role in proliferation, tumorigenesis, metastasis, and stemness (33, 34). A common tumor-associated antigen, EpCAM is frequently used as a diagnostic marker for various cancers and as a target for novel immunotherapies. Interestingly, the influence of EpCAM on ENT1 expression, localization and activity superintended the contribution of cadherin switching. Mechanistically, EpCAM overexpression also increased E-cadherin expression in mesenchymal pancreatic cancer cells and exerted a negative effect on N-cadherin expression at the cell surface. Therefore, it is likely that EpCAM supports ENT1 cell surface expression in an indirect manner by opposing cadherin switching. Indeed, previous reports identify the ability of EpCAM to modulate adhesion mediated by classical cadherins (35, 36). Functionally, we observed overexpression of EpCAM did not significantly alter ENT1 transport in PANC-1 cells, which express endogenous E-cadherin and displayed heterogeneous patterns of EpCAM overexpression. On the other hand, uniform EpCAM overexpression was noted in N+/E− cells with a highly significant increase in gemcitabine accumulation. We speculate that other factors such as drug efflux, metabolism, or the crosstalk between E-cadherin and EpCAM molecules may minimize or mask changes in gemcitabine transport in the PANC-1 cell line, which contains an assortment of phenotypes. Overall, our findings identify a loss of EpCAM during EMT resulting in decreased membrane ENT1 expression and sensitivity to nucleoside analog drugs, suggesting a new function of this multifunctional protein in epithelial pancreatic cancer cells.

Unlike the role of EMT in chemoresistance, the contribution of EMT to metastasis formation in pancreatic cancer is still under debate (9, 11). Zheng and colleagues showed that Snail- or Twist-induced EMT is not rate-limiting for invasion and metastasis in pancreatic cancer, (11) yet contrasting studies uphold the role of EMT acting as a prerequisite for tumor spread and metastatic development (9). Both epithelial and mesenchymal-type tumor cells, along with intermediate EMT phenotypes, are potentially able to seed new tumors. Interestingly, Liu and colleagues recently showed that circulating tumor cells with predominantly epithelial

and lesser mesenchymal traits were most capable of generating secondary tumors in breast cancer (8).Other evidence suggests that a fraction of circulating tumor cells shed EpCAM expression due to EMT which may contribute to increased metastasis with chemoresistance (15). Our findings demonstrate that epithelial-type cells, as characterized by expression of EpCAM and E-cadherin, are sensitive to treatment with gemcitabine due to retained cell surface expression of ENT1. Thus, it is likely that mesenchymal cells or circulating tumor cells that have undergone EMT may evade drug therapy by loss of ENT1 transport facilitated at least partially by N-cadherin expression. Although the predominantly epithelial cells may be able to form tumors at the highest rate, if such cells are eliminated by drug treatment, the mesenchymal cells that escape therapy still have the potential to generate metastasis. The reduced metastatic incidence and improved drug response in mice harboring orthotopic pancreatic cancer cells that overexpress EpCAM, but not N-cadherin, lends support to this possibility. Further, the link that our study establishes between loss of ENT1 and the EMT process suggests that primary tumor EMT characteristics may be a useful predictor of response to nucleoside analog drugs. Histopathological methods for that assess EMT status and/or ENT1 membrane function which is compromised during EMT could inform on the selection of chemotherapeutic agents. Thus, treatment with nucleoside analog drugs may not be appropriate for patients with significant evidence of EMT.

Several groups have reported loss of ENT1 as predictive of worsened outcomes in pancreatic cancer (37–39), however, inconsistencies were noted in some studies with lack of correlation between ENT1 expression and treatment outcomes (40, 41). Our study examined not only the intensity of ENT1 expression in patient samples, but also the subcellular distribution of ENT1, and found that cell surface ENT1 positively predicted gemcitabine-treated patient survival. These results indicate that both expression and localization of ENT1 are important predictors of patient response to nucleoside analog treatment, perhaps explaining some of the inconsistencies noted earlier. Such an analysis performed prospectively on biopsied PDAC samples would allow for the identification of an ENT1 subtyping index to be incorporated into routine diagnostics for better prediction of gemcitabine drug response in patients. These results also suggest that administration of nucleoside analog drugs combined with a therapeutic agent to suppress EMT may reduce gemcitabine drug resistance in PDAC.

In summary, our findings identify that functional loss of ENT1 during EMT drives gemcitabine resistance in pancreatic cancer cells. The findings identify a putative mechanism by which mesenchymal-type cells evade nucleoside analog chemotherapy and may have predictive value in the treatment of pancreatic cancer patients.

Supplementary Material

Refer to Web version on PubMed Central for supplementary material.

ACKNOWLEDGEMENTS

We are grateful for the assistance with confocal microscopy and image processing provided by Dr. Sara Cole and Brian Kemmenoe of the Campus Microscopy and Imaging Facility, The Ohio State University. We thank Anusha Singh and Shreya Barde for their contribution to the immunostaining experiments and Ryan Robb for the assistance with TMA image analysis.

FINANCIAL INFORMATION

This work was supported by the awards NIH 1R01CA188464 (RG) and NIH 1R01CA198128 (TMW), and by Research Scholars Grants, RSG-15-036-01-DDC (RG) and RSG-17-221-01-TBG (TMW) from the American Cancer Society. DN and AKP were supported by the Ohio State University Comprehensive Cancer Center Pelotonia Fellowship Program.

Images presented in this report were generated using the instruments and services at the Campus Microscopy and Imaging Facility, The Ohio State University. This facility is supported in part by grant P30 CA016058, National Cancer Institute, Bethesda, MD.

REFERENCES

1. Howlader N, Noone AM, Krapcho M, Miller D, Brest A, Yu M, et al. SEER Cancer Statistics Review, 1975–2016, National Cancer Institute. Bethesda, MD, based on November 2018 SEER data submission, posted to the SEER web site, April 2019.
2. Conroy T, Desseigne F, Ychou M, Bouche O, Guimbaud R, Becouarn Y, et al. FOLFIRINOX versus gemcitabine for metastatic pancreatic cancer. N Engl J Med 2011;364:1817–1825. [PubMed: 21561347]
3. Sohal DP, Mangu PB, Khorana AA, Shah MA, Philip PA, O'Reily EM, et al. Metastatic Pancreatic Cancer: American Society of Clinical Oncology Clinical Practice Guideline. J Clin Oncol 2016; 34,23:2784–96. [PubMed: 27247222]
4. Siegel RL, Miller KD, Jemal A. Cancer statistics, 2019. CA Cancer J Clin. 2019;69(1):7–34. [PubMed: 30620402]
5. Mani SA, Guo W, Liao MJ, Eaton EN, Ayyanan A, Zhou AY, et al. The epithelial-mesenchymal transition generates cells with properties of stem cells. Cell 2008; 133(4), 704–715. [PubMed: 18485877]
6. Lim J, Thiery JP. Epithelial-mesenchymal transitions: insights from development. Development. 2012;139(19):3471–86. [PubMed: 22949611]
7. Yu M, Bardia A, Wittner BS, Stott SL, Smas ME, Ting DT, et al. Circulating breast tumor cells exhibit dynamic changes in epithelial and mesenchymal composition. Science. 2013;339(6119):580–4. [PubMed: 23372014]
8. Liu X, Li J, Cadilha BL, Markota A, Voigt C, Huang Z, et al. Epithelial-type systemic breast carcinoma cells with a restricted mesenchymal transition are a major source of metastasis. Sci Adv. 2019;5:eaav4275.
9. Rhim AD, Mirek ET, Aiello NM, Maitra A, Bailey JM, McAllister F, et al. EMT and dissemination precede pancreatic tumor formation. Cell 2012;148(1–2), 349–361. [PubMed: 22265420]
10. Katsuno Y, Meyer DS, Zhang Z, Shokat KM, Akhurst RJ, Miyazono K, et al. Chronic TGF-β exposure drives stabilized EMT, tumor stemness, and cancer drug resistance with vulnerability to bitopic mTOR inhibition. Science signaling 2019;12(570):eaau8544.
11. Fischer KR, Durrans A, Lee S, Sheng J, Li F, Wong ST, et al. Epithelial-to-mesenchymal transition is not required for lung metastasis but contributes to chemoresistance. Nature 2015;527(7579):472–6. [PubMed: 26560033]
12. Zheng X, Carstens JL, Kim J, Scheible M, Kaye J, Sugimoto H, et al. Epithelial-to-mesenchymal transition is dispensable for metastasis but induces chemoresistance in pancreatic cancer. Nature 2015;527(7579):525–530. [PubMed: 26560028]
13. Arumugam T, Ramachandran V, Fournier KF, Wang H, Marquis L, Abbruzzese JL, et al. Epithelial to mesenchymal transition contributes to drug resistance in pancreatic cancer. Cancer Res, 2009;69(14):5820–5828. [PubMed: 19584296]
14. Izumchenko E, Chang X, Michailidi C, Kagohara L, Ravi R, Paz K, et al. The TGFβ-miR200-MIG6 pathway orchestrates the EMT-associated kinase switch that induces resistance to EGFR inhibitors. Cancer Res 2014;74(14):3995–4005 [PubMed: 24830724]
15. Meng Q, Shi S, Liang C, Liang D, Hua J, Zhang B, et al. Abrogation of glutathione peroxidase-1 drives EMT and chemoresistance in pancreatic cancer by activating ROS-mediated Akt/GSK3β/Snail signaling. Oncogene 2018;37(44):5843–5857. [PubMed: 29980787]

16. Huang RY, Guilford P, Thiery JP. Early events in cell adhesion and polarity during epithelial-mesenchymal transition. J Cell Sci. 2012;125:4417–22. [PubMed: 23165231]
17. Wheelock MJ, Shintani Y, Maeda M, Fukumoto Y, Johnson KR. Cadherin switching. J Cell Sci 2008;121:727–35. [PubMed: 18322269]
18. Gorges TM, Tinhofer I, Drosch M, Röse L, Zollner TM, Krahn T, et al. Circulating tumour cells escape from EpCAM-based detection due to epithelial-to-mesenchymal transition. BMC Cancer 2012;12:178. [PubMed: 22591372]
19. Qi LN, Xiang BD, Wu FX, Ye JZ, Zhong JH, Wang YY, et al. Circulating Tumor Cells Undergoing EMT Provide a Metric for Diagnosis and Prognosis of Patients with Hepatocellular Carcinoma. Cancer Res 2018;78(16):4731–4744. [PubMed: 29915159]
20. Chakraborty S, Mitra S, Falk MM, Caplan SH, Wheelock MJ, Johnson KR, et al. E-cadherin differentially regulates the assembly of Connexin43 and Connexin32 into gap junctions in human squamous carcinoma cells. J Biol Chem 2010;285(14):10761–76. [PubMed: 20086013]
21. Bhutia YD, Hung SW, Patel B, Lovin D, Govindarajan R. CNT1 expression influences proliferation and chemosensitivity in drug-resistant pancreatic cancer cells. Cancer Res. 2011;71(5):1825–35. [PubMed: 21343396]
22. García-Manteiga J, Molina-Arcas M, Casado FJ, Mazo A, Pastor-Anglada M. Nucleoside transporter profiles in human pancreatic cancer cells: role of hCNT1 in 2',2'-difluorodeoxycytidine- induced cytotoxicity. Clin Cancer Res 2003 Oct;9(13):5000–8. [PubMed: 14581375]
23. Hioki M, Shimada T, Yuan T, Nakanishi T, Tajima H, Yamazaki M, et al. Contribution of equilibrative nucleoside transporters 1 and 2 to gemcitabine uptake in pancreatic cancer cells. Biopharm Drug Dispos 2018;39(5):256–64. [PubMed: 29682747]
24. Mangravite LM, Xiao G, Giacomini KM. Localization of human equilibrative nucleoside transporters, hENT1 and hENT2, in renal epithelial cells. Am J Physiol Renal Physiol 2003;284(5):F902–10. [PubMed: 12527552]
25. Takahashi K, Ehata S, Koinuma D, Morishita Y, Soda M, Mano H, et al. Pancreatic tumor microenvironment confers highly malignant properties on pancreatic cancer cells. Oncogene. 2018;37(21):2757–72. [PubMed: 29511349]
26. Govindarajan R, Chakraborty S, Johnson KE, Falk MM, Wheelock MJ, Johnson KR, et al. Assembly of Connexin43 into Gap Junctions Is Regulated Differentially by E-Cadherin and N-Cadherin in Rat Liver Epithelial Cells. Mol Biol Cell. 2010 Dec 1;21(23):4089–107. [PubMed: 20881055]
27. Hagmann W, Jesnowski R, & Löhr JM. Interdependence of gemcitabine treatment, transporter expression, and resistance in human pancreatic carcinoma cells. Neoplasia 2010;12(9):740–747. [PubMed: 20824050]
28. Nieto MA, Huang RY, Jackson RA, Thiery JP. EMT: 2016. Cell 2016;166(1):21–45. [PubMed: 27368099]
29. Batlle E, Sancho E, Francí C, Domínguez D, Monfar M, Baulida J, et al. The transcription factor snail is a repressor of E-cadherin gene expression in epithelial tumour cells. Nat Cell Biol 2000;2:84–89. [PubMed: 10655587]
30. Yang H, Wang L, Zhao J, Chen Y, Lei Z, Liu X, et al. TGF-β-activated SMAD3/4 complex transcriptionally upregulates N-cadherin expression in non-small cell lung cancer. Lung Cancer 2015;87:249–257. [PubMed: 25595426]
31. Menke A, Philippi C, Vogelmann R, Seidel B, Lutz MP, Adler G, et al. Down-regulation of E-cadherin gene expression by collagen type I and type III in pancreatic cancer cell lines. Cancer Res. 2001;61(8):3508–17. [PubMed: 11309315]
32. Nivillac NMI, Bacani J, Coe IR. The life cycle of human equilibrative nucleoside transporter 1: From ER export to degradation. Experimental Cell Research. 2011 Jul 1;317(11):1567–79. [PubMed: 21402067]
33. Munz M, Baeuerle PA, Gires O. The Emerging Role of EpCAM in Cancer and Stem Cell Signaling. Cancer Res 2009;69(14):5627. [PubMed: 19584271]
34. Maetzel D, Denzel S, Mack B, Canis M, Went P, Benk M, et al. Nuclear signalling by tumour-associated antigen EpCAM. Nat Cell Biol 2009;11(2):162–71. [PubMed: 19136966]

35. Litvinov SV, Balzar M, Winter MJ, Bakker HA, Briaire-de Bruijn IH, Prins F, et al. Epithelial cell adhesion molecule (Ep-CAM) modulates cell-cell interactions mediated by classic cadherins. J Cell Biol 1997;139(5):1337–1348. [PubMed: 9382878]

36. Guerra E, Lattanzio R, La Sorda R, Dini F, Tiboni GM, Piantelli M, et al. mTrop1/Epcam Knockout Mice Develop Congenital Tufting Enteropathy through Dysregulation of Intestinal E-cadherin/β-catenin. PLoS One 2012;7(11).

37. Lai R, Mackey JR. The absence of human equilibrative nucleoside transporter 1 is associated with reduced survival in patients with gemcitabine-treated pancreas adenocarcinoma. Clin Cancer Res 2004;10(20):6956–61. [PubMed: 15501974]

38. Giovannetti E, Del Tacca M, Mey V, Funel N, Nannizzi S, Ricci S, et al. Transcription analysis of human equilibrative nucleoside transporter-1 predicts survival in pancreas cancer patients treated with gemcitabine. Cancer Res 2006;66(7):3928–35. [PubMed: 16585222]

39. Liu ZQ, Han YC, Zhang X, Chu L, Fang JM, Zhao HX, et al. Prognostic value of human equilibrative nucleoside transporter1 in pancreatic cancer receiving gemcitabine-based chemotherapy: a meta-analysis. PloS one 2014;9,1 e87103.

40. Svrcek M, Cros J, Maréchal R, Bachet J-B, Fléjou J-F, Demetter P. Human equilibrative nucleoside transporter 1 testing in pancreatic ductal adenocarcinoma: a comparison between murine and rabbit antibodies. Histopathology. 2015 Feb;66(3):457–62. [PubMed: 25298108]

41. Sinn M, Riess H, Sinn BV, Stieler JM, Pelzer U, Striefler JK, et al. Human equilibrative nucleoside transporter 1 expression analysed by the clone SP 120 rabbit antibody is not predictive in patients with pancreatic cancer treated with adjuvant gemcitabine – Results from the CONKO-001 trial. European Journal of Cancer. 2015 Aug 1;51(12):1546–54. [PubMed: 26049689]

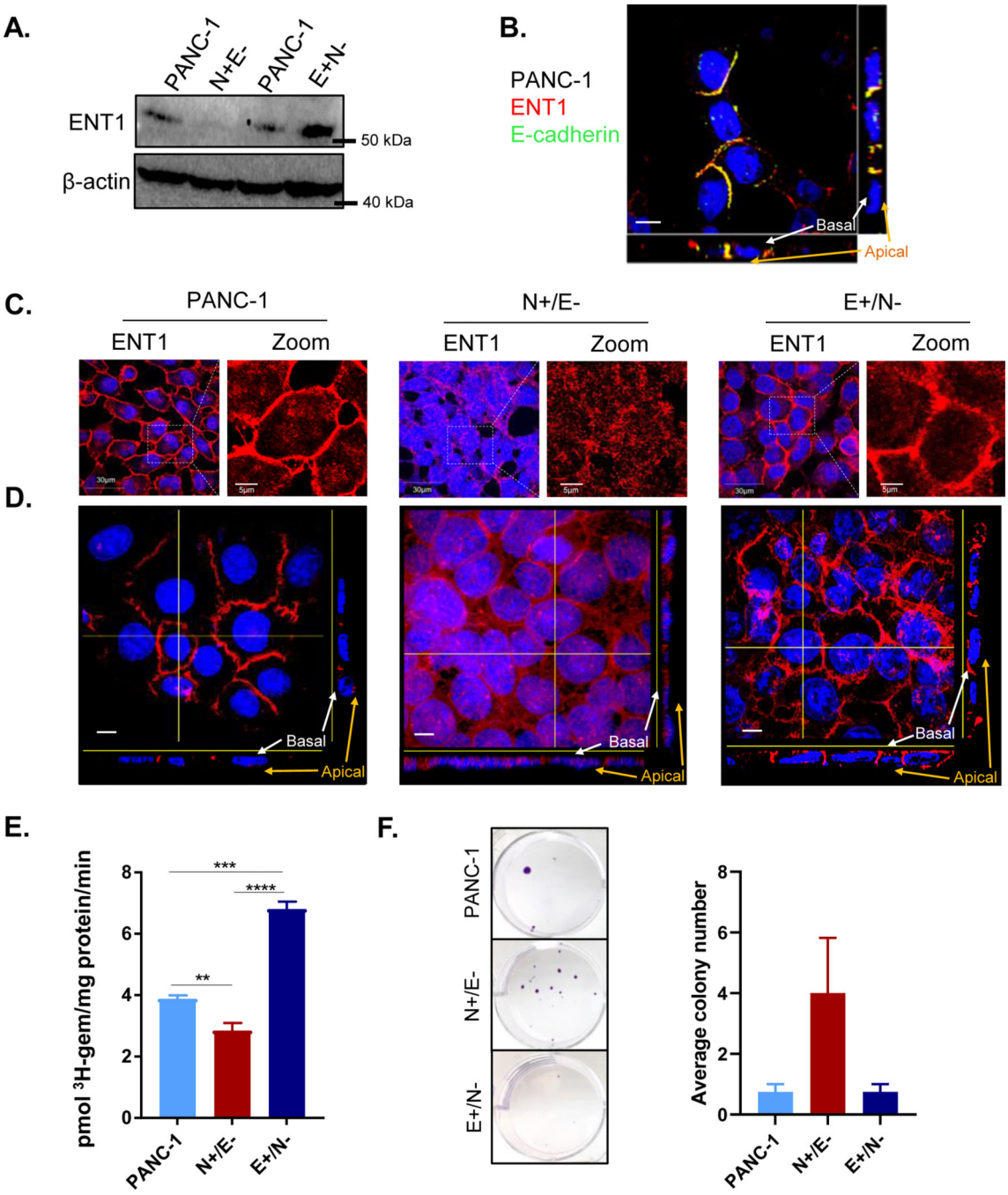

Figure 1: ENT1 is decreased in mesenchymal subclones derived from PANC-1 cells

A. Western blotting analysis of total hENT1 protein levels in PANC-1 cells compared to N+/E− and E+/N− cells with β-actin as a loading control B. ENT1 (red) and E-cadherin (green) and merged images show colocalization at the lateral membrane (yellow) of PANC-1 cells; Bar= 10 μM C. Confocal micrograph of immunocytochemical analysis of hENT1 (red) in a single z-slice. Right panel shows magnified view of ENT1 localization. Original magnification, x60 D. Z-intensity projection of confocal micrographs captured show hENT1 localization throughout the entire cell. Yellow lines show placement of

transverse segment that corresponds with orthogonal view displayed at the bottom and to the right of the composite image. Original magnification, x100; bar, 10 μm E. Total transport of ^{3}H-gemcitabine (1 μM) in sodium containing buffer for each cell type. Bars, means ± SD (n=3) Statistical analyses were performed with two-tailed Student's t-test. **P≤0.01, ***P≤0.001, ****P≤0.0001 F. Crystal violet staining shows colony formation assay. Cells were seeded at equivalent number and grown in the presence of 10 nM gemcitabine for 3 weeks prior to fixation and staining.

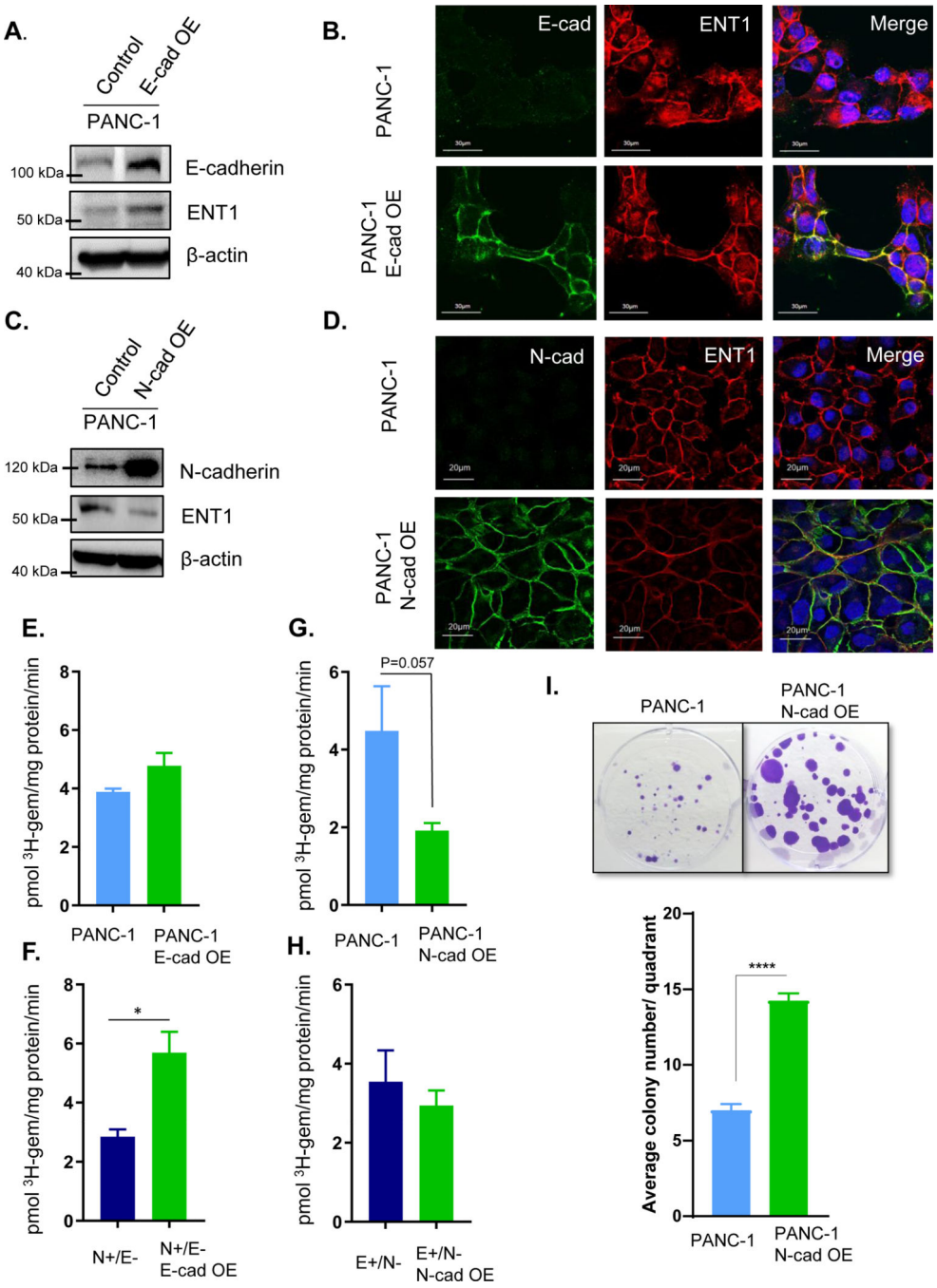

Figure 2: Cadherin switching diminishes ENT1 cell surface localization and function

A. Western blot analysis shows overexpression (OE) of E-cadherin in PANC-1 cells and ENT1 protein levels. β-actin is used as an internal control B. Immunostaining for E-cadherin is shown in green (left), hENT1 in red (middle), and both channels merged with DAPI (right). Original magnification, x60 C. ENT1 protein levels were examined by Western blotting in control and PANC-1 N-cadherin OE cells; OE= overexpression. β-actin is used as an internal control D. Confocal micrographs display co-immunostaining for N-cadherin in green, ENT1 in red, and merged with nuclear counterstain DAPI E.-H. Transport of ^{3}H-

gemcitabine (1 μM) in sodium containing buffer for each cell type measured for 1 minute. Bars, means ± SD (n=3). Statistical analyses were performed with two-tailed Student's t-test. I. Colony formation ability of PANC-1 and PANC-1 cells overexpressing N-cadherin was performed by seeding equivalent cell number and treating with 10 nM gemcitabine for 3 weeks prior to staining with crystal violet to visualize colonies. Quantification was performed by counting the number of colonies ≥1 mm in size for each quadrant of the 6-well plate and averaging for the entire well. Bars= mean ± SEM. Statistical analyses were performed with two-tailed Student's t-test. *P ≤ 0.05, ****P ≤ 0.0001

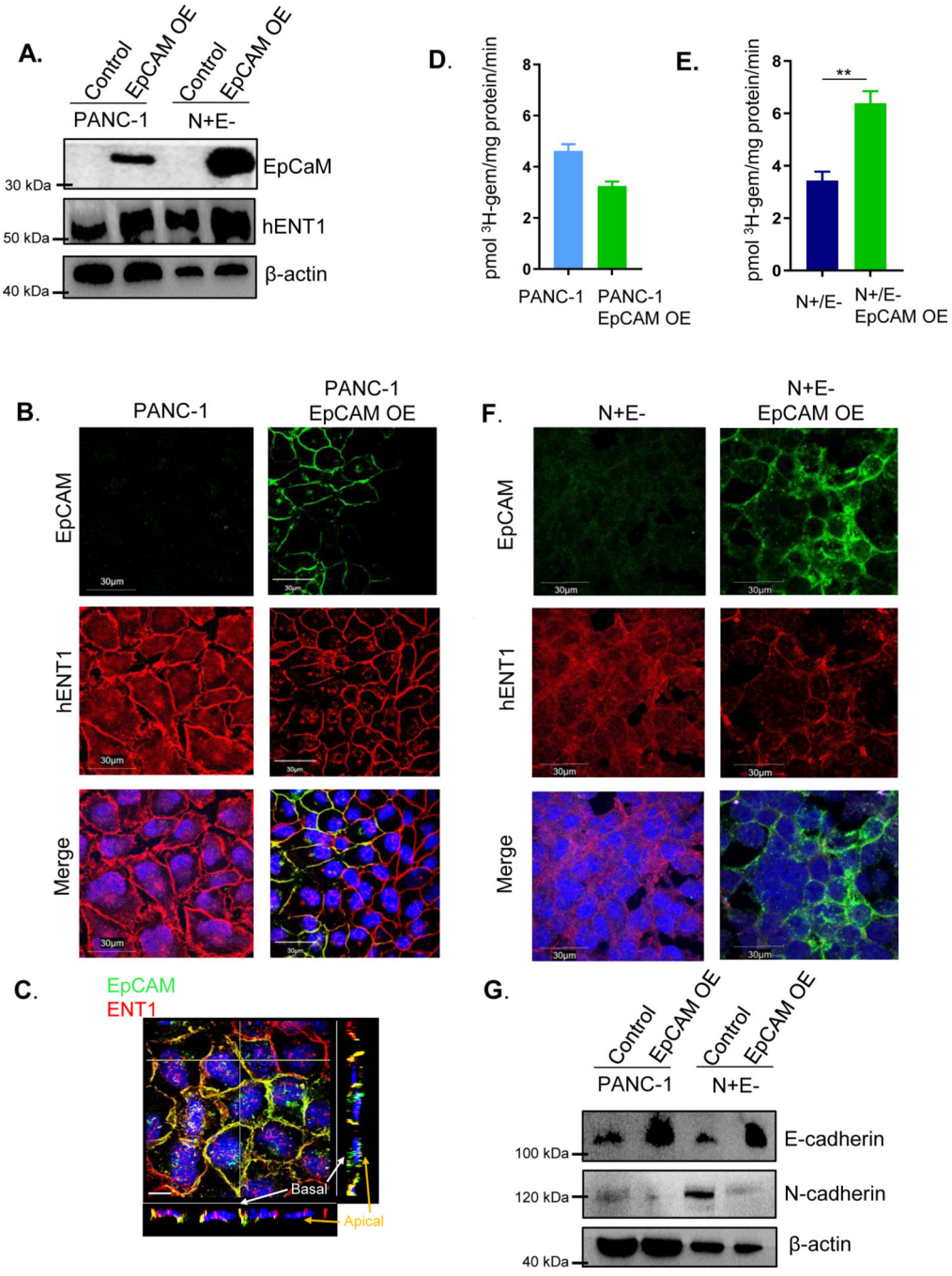

Figure 3: EpCAM opposes cadherin switching and stabilizes ENT1 at the cell surface

A. Western blotting analysis of hENT1, EpCAM, N-cadherin, and E-cadherin expression following stable retroviral overexpression of EpCAM in PANC-1 and N+/E− cells. β-actin is used as an internal loading control. OE, overexpression. B. Immunostaining for EpCAM (green) and hENT1 (red) in PANC-1 control and PANC-1 overexpressing EpCAM. C. Z-intensity projection of compiled confocal micrographs show ENT1 (red) and EpCAM (green) localization throughout entire cells. Yellow transverse lines indicate position of slices where orthogonal view is shown at the bottom and to the right of the image and

Z-projection 3D perspective view at 45° from horizontal; Bar, 10 μm. D. Immunostaining for EpCAM (green) and hENT1 (red) in N+/E− and N+/E− cells overexpressing EpCAM E./F. Transport of ^{3}H-gemcitabine (1 μM) in PANC-1 and N+/E− cells stably expressing EpCAM conducted using sodium containing buffer. Bars, means ± SD (n=3). Statistical analyses were performed with two-tailed Student's t-test. *P ≤ 0.05, **P ≤ 0.01

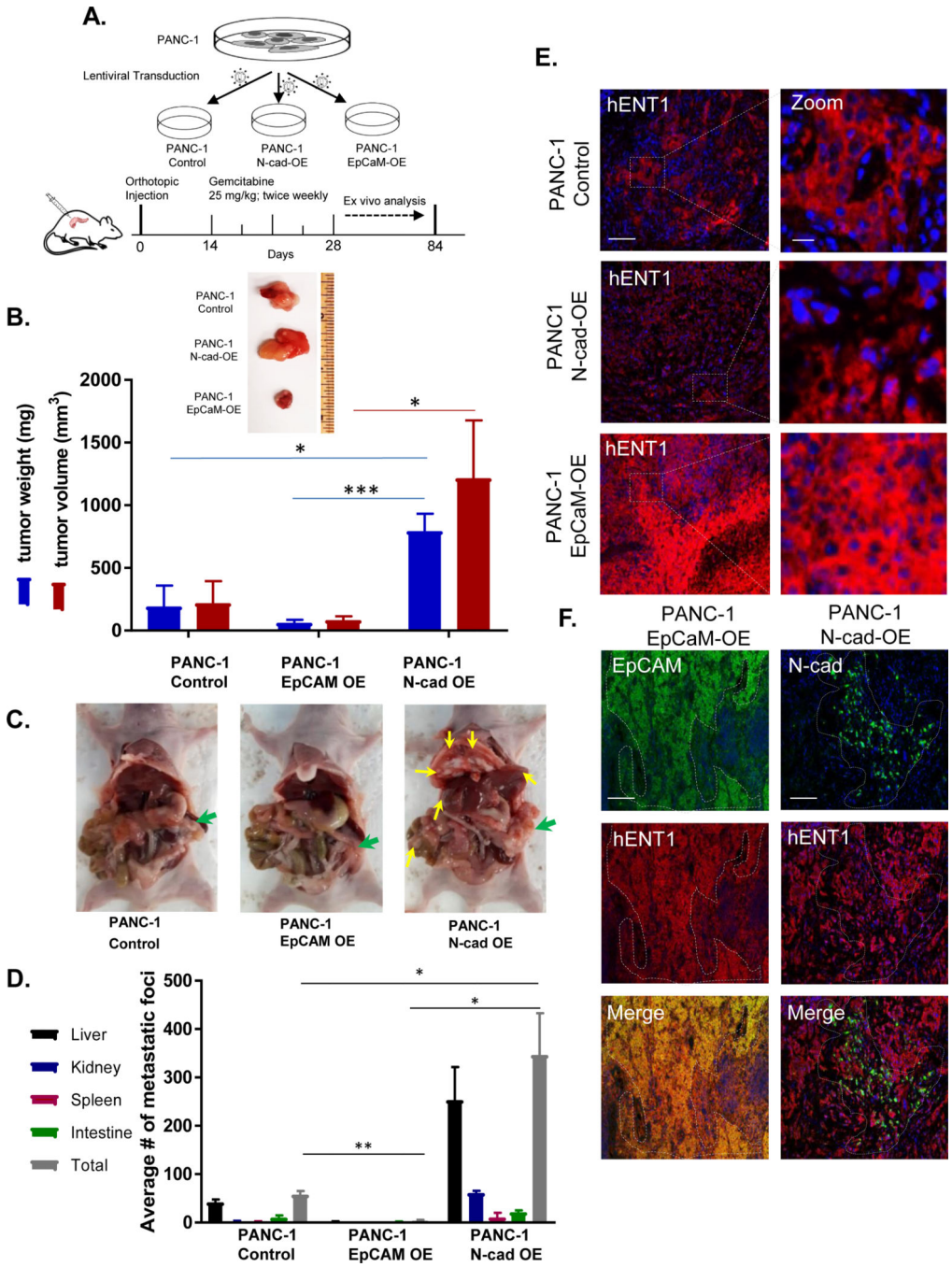

Figure 4: N-cadherin-expressing tumors evade gemcitabine treatment in a pancreatic cancer orthotopic mouse model

A. Schematic representation of pancreatic orthotopic mouse tumor study for the evaluation of N-cadherin or EpCAM effects on gemcitabine therapy. PANC-1, PANC-1 overexpressing N-cadherin, or PANC-1 overexpressing EpCAM cells were orthotopically injected into the pancreas of immunodeficient female nude mice and gemcitabine treatment initiated two weeks after the engraftment procedure for the duration of the study. After 12 weeks, all mice were euthanized, and tumor burden and metastases incidence were evaluated *ex vivo*. B. Representative primary tumor from each group showing relative size and quantification of

tumor volume and weight; OE, overexpression. Bars, mean ± SEM (n=5/group) C. Mouse necropsies showing primary tumors in pancreas (green arrows) and metastatic nodules in secondary sites (yellow arrows.) D. Bar graph shows average number of metastatic nodules in vital abdominal organs E. Immunohistochemical analysis of hENT1 was performed for primary tumors. Representative images of hENT1 (red) expression and nuclear counterstain DAPI (blue) in different groups (left) and zoomed in to show detail (right). Bar, 100 μm. Zoom bar, 10 μm. F. Immunohistochemical analysis in primary tumors for hENT1 (red) and EpCAM (green) (left) or hENT1 (red) and N-cadherin (green) (right) with merged images depicting coexpression (yellow). Bar, 100 μm. Statistical analyses performed with two-tailed Student's t-test. *P ≤ 0.05, **P ≤ 0.01, ***P ≤ 0.001

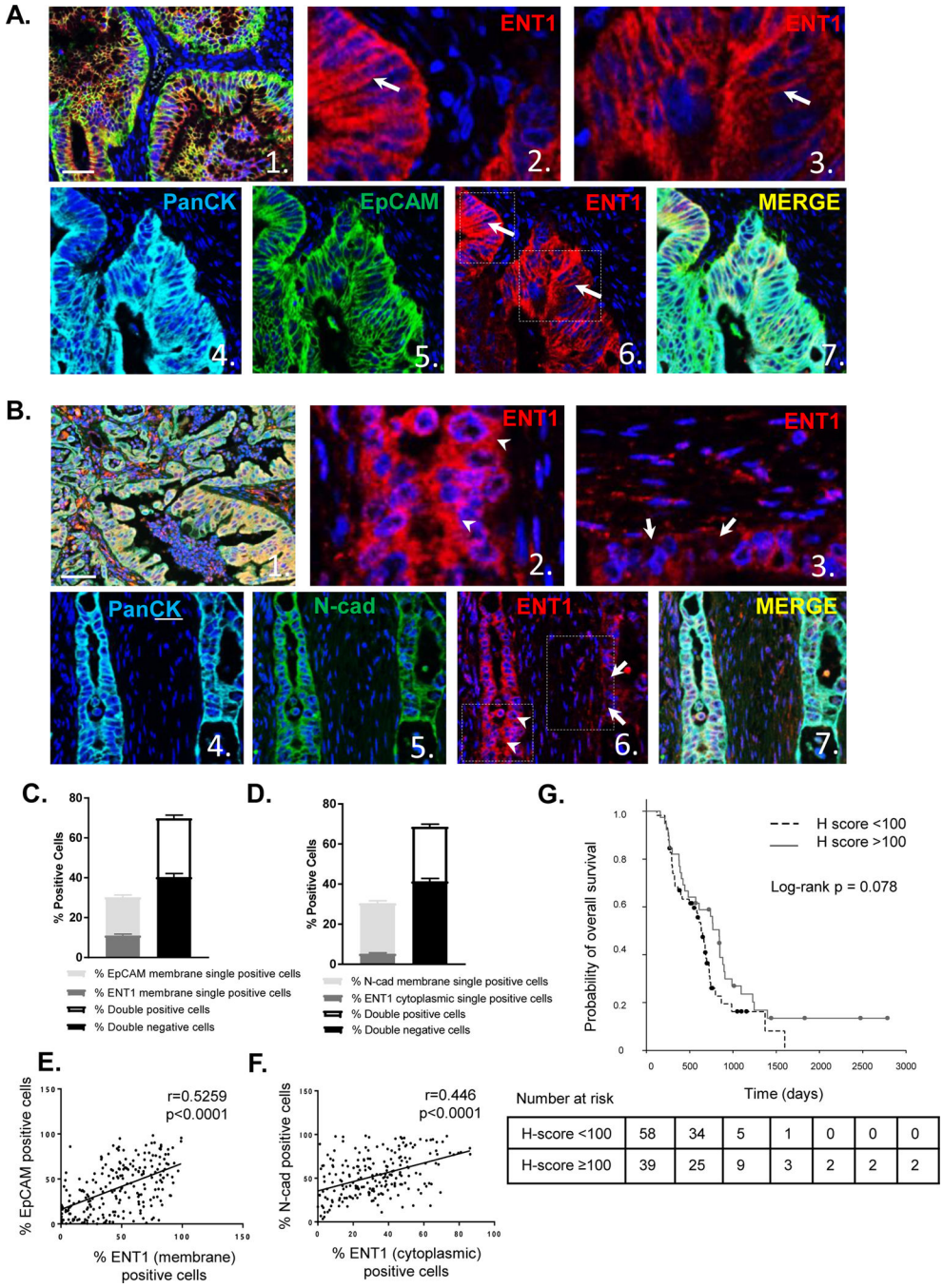

Figure 5: EpCAM determines ENT1 localization in human pancreatic cancer and cell surface localization of ENT1 positively predicts median overall survival

A. Representative multi-spectral fluorescent images of pancreatic cancer TMA sample stained for ENT1 (red), Pan-Cytokeratin (cyan), and EpCAM (green) with nuclear counterstain DAPI. Image 1. shows a composite image at 20x magnification (bar, 50 μm), while images 2. and 3. show a zoom view of image 6. ENT1 localization at the plasma membrane. Images 4. and 5. display single channel views of Pan-Cytokeratin and EpCAM respectively with a merged view shown in 7. Expression of Pan-cytokeratin segments tumor cells from surrounding stroma. B. Example images of TMA sample stained

for ENT1 (red), Pan-cytokeratin (cyan), and N-cadherin (green) shown in the same order as EpCAM representation C. Tumor cells were segmented into nuclear, cytoplasmic and plasma membrane compartments with Inform software (see supplemental methods), and cells were counted for plasma membrane expression of EpCAM and plasma membrane ENT1 single and double positivity/negativity D. Plasma membrane N-cadherin and cytosolic ENT1 plasma membrane single and double positivity/negativity. Graphs show average percentage of cells in each category for all patients (n=114); Bars, mean ±SD E. Scatter plots show correlation between percentage of EpCAM plasma membrane-positive cells and ENT1 plasma membrane-positive cells F. Correlation between percentage of N-cadherin plasma membrane-positive cells and ENT1 cytoplasmic-positive cells G. Median overall survival time for gemcitabine-based chemotherapy treated patients (n=97) segregated by H-score which represents intensity of ENT1 plasma membrane staining between 0 and 300, with 0 indicating no expression of ENT1 and 300 indicating maximal expression of ENT1. Threshold value for high/low ENT1 expression was 100 based on the median H-score, 96.1. Number of patients at risk at each time point is listed for each group below the survival curve.

Table 1.

Univariate and multivariate Cox proportional hazard survival analyses of overall survival

Factor	Hazard ratio	195% CI of HR	P value
Univariate			
Age Increasing by 1	0.99	[0.97, 1.01]	0.42
Gender female *vs* male	0.83	[0.55, 1.27]	0.4
Adjuvant chemotherapy yes *vs* no	0.48	[0.28, 0.81]	0.0065
H-score > 100 *vs* < 100	0.68	[0.45, 1.05]	0.078
Grade 3 *vs* (1 and 2)	1.5	[0.97, 2.30]	0.067
N stage 1 *vs* 0	2.53	[1.39, 4.57]	0.0022
T stage (3 and 4) *vs* (1 and 2)	5.12	[1.61, 16.33]	0.0058
LVSI positive *vs* negative	0.65	[0.42, 1.03]	0.065
PNI positive *vs* negative	0.75	[0.45, 1.25]	0.28
Surgical margin status positive *vs* negative	1.87	[1.21, 2.88]	0.0047
Multivariate *			
Adjuvant chemotherapy yes *vs* no	0.45	[0.26, 0.78]	0.0042
ENT1 H-score > 100 *vs* < 100	0.7	[0.45, 1.03]	0.09
N stage 1 *vs* 0	2.33	[1.27, 4.25]	0.006

* the overall p value of the final multivariate model was less than 0.001 (log-rank test)

Univariate and multivariate survival analyses were conducted to evaluate the potential associations between H-score, adjuvant chemotherapy treatment, tumor grade, N stage, T stage, lymphovascular space invasion (LVSI), perineural invasion (PNI), surgical margin status, and median overall survival. The multivariate analyses were performed using a stepwise backward approach. Due to the relatively small sample size, the final multivariate model included variables with p value < 0.10.